Electrical Power and Energy Systems 45 (2013) 167–174

Contents lists available at SciVerse ScienceDirect

Electrical Power and Energy Systems

journal homepage: www.elsevier.com/locate/ijepes

Loadability of power systems and optimal SVC placement

J.S. Huang [a,*], Z.H. Jiang [a], M. Negnevitsky [b]

[a] School of Computing, Engineering and Mathematics, University of Western Sydney, Locked Bag 1797, Penrith, NSW 2751, Australia
[b] School of Engineering, University of Tasmania, Hobart, Tasmania 7001, Australia

ARTICLE INFO

Article history:
Received 20 December 2007
Received in revised form 27 August 2012
Accepted 29 August 2012
Available online 11 October 2012

Keywords:
SVC placement
Worst-case reactive power margin
$N-1$ security criterion
Messy genetic algorithm
Lagrange multiplier method
Fuzzy logic performance index

ABSTRACT

This paper investigates the loadability of power systems. A voltage stability assessment is performed using the worst-case reactive power margin as an index. In addition, the influence of active power load increment on the voltage stability assessment is also examined. Based on these results, a messy genetic-algorithm optimization scheme is proposed for optimal static VAR compensator (SVC) placement aimed at the voltage stability enhancement of power systems under the most critical operation conditions. The SVC planning is formulated as a multi-objective optimization problem in terms of the maximum worst-case reactive power margin, highest load voltages towards the critical operating points, minimum real power losses, and lowest SVC device costs. During the genetic algorithm search for the optimal solution, the most critical disturbance scenario is estimated using each SVC placement and the configuration of the original power system. The candidate solution thereby obtained is further checked against the $N-1$ security criterion.

1. Introduction

Recent years have witnessed quite a number of large-scale blackouts of power systems, among which, voltage instability is one of the main reasons leading to the outage [1–4]. While voltage stability is affected by factors such as voltage regulation, reactive power compensation and management, rotor angle stability, protective relaying and control center operations, it can be regarded as a phenomenon associated with inability of power systems to meet reactive load demands, which may be owing to inadequate VAR supports or violation of reactive power transmission limits [4]. From the viewpoint of security, the load demands of a power system should be restricted within a range to maintain certain reactive reserve. Otherwise the power system may be unable to sustain a desired voltage profile and become unstable even under small disturbances. Intuitively, the reactive loadability, or the reactive power margin can be used to define a proximity index of voltage stability [5,6].

One possible method of evaluating the reactive loadability is to stress the power system by increasing the loads progressively and perform the load flow calculation at each step. Unless some modifications are made to conventional load flow programs, this method may fail to find the exact critical point due to the numerical problem. The other more sophisticated alternative is to directly locate the critical point by solving an optimization problem, which is much more efficient and accurate by taking into account various control variables and operating constraints. The method seeks the reactive loadability by maximizing the loads in the whole or a specified area of the power system. A number of algorithms based on nonlinear programming or the like techniques have been developed for solving such type of optimization [7–9]. The maximum loadability method has a clear physical meaning and the estimation results can be directly applied in planning and operating power systems. However, existing methods contain certain limitations. They were either based on simplified power flow models thus inadequate in considering some pertinent constraints, or assumed specified disturbance modes without reflecting the most critical operation conditions.

Since the capability of a power system to transfer reactive power from production sources to consumption sinks during steady operating conditions is a primary requirement to avoid voltage instability, static VAR compensators (SVCs) have been widely used in electric power systems, and SVC planning therefore has been a major concern of power utilities. Up to date, significant efforts have been engaged in this field with most of the developed methods addressing optimal VAR placement with respect to voltage and reactive power [10–16].

Because voltage stability is associated with reactive power support, for voltage stability reinforcement, therefore, the optimal SVC placement can be obtained by seeking a compensation scheme that maximizes the system reactive power margin. Transmission limits of feeders are another main reason resulting in voltage instability. Likewise, operating limits may be exceeded due to line overloading before draining of reactive power reserves. Guarding against feeder

* Corresponding author.
E-mail addresses: j.huang@uws.edu.au (J.S. Huang), z.jiang@uws.edu.au (Z.H. Jiang), Michael.Negnevitsky@utas.edu.au (M. Negnevitsky).

0142-0615/$ - see front matter Crown Copyright © 2012 Published by Elsevier Ltd. All rights reserved.
http://dx.doi.org/10.1016/j.ijepes.2012.08.064

line overloads through minimizing real power losses is thus important in SVC planning, not only for the benefits of economical operation but also for security considerations. Yet another cause of voltage instability is voltage sags. In addition to power quality problems, voltage sags can directly bring about voltage collapse of power systems [4]. Hence, ability of a power system in maintaining load voltages is taken into account in the SVC planning. As done by most of the planning problems, the minimum cost of the SVC scheme is taken as one of the objectives as well. The $N-1$ criterion in SVC placement expresses the ability of a power system to lose a transmission line without causing voltage instability elsewhere. Apart from the above considerations, therefore, the SVC placement should also ensure a certain $N-1$ reactive power margin.

This paper extends authors' previous work [7,10] to investigate the maximum loadability by employing the full power flow model of power systems. The voltage stability is performed in terms of the worst-case reactive power margins with or without incremental active power demands. Based on the defined voltage stability index, SVC planning is conducted aiming at the optimal placement for voltage stability reinforcement under the most critical operation states, including the $N-1$ security criterion.

The paper is organized as follows. Section 2 investigates the loadability of a power system. By stressing the power system with extra active and reactive power demands, the most critical disturbance scenario and the associated worst-case reactive power margin of a power system is identified. Section 3 discusses closed related factors in voltage stability analysis, formulates four sub-objectives and defines a fuzzy performance index for the SVC placement. The $N-1$ reactive power margin is also discussed in this section to assess the performance of the candidate SVC placement in this regard. Section 4 describes the optimization techniques of nonlinear programming and the messy genetic algorithm (GA) adopted in this research. Numeric simulations and discussions are given in Section 5. Section 6 concludes the paper.

2. Loadability of a power system

Voltage collapse and related instability problems can be caused by single or simultaneous occurrence of unusual conditions such as unexpected load increase, loss of important transmission lines, transformers, or generators, and inappropriate actions of control devices. In most if not all of these cases, voltage instability is characterized by inadequate reactive supports either system-wide or locally. For secure operations, power systems must remain stable following these unusual conditions. Otherwise, load demands may have to be curtailed in order to maintain sufficient reactive reserve so as to withstand even a small disturbance. Estimating the reactive power margin is thus an important task in monitoring power systems' operation. In evaluating the system VAR margin, conventional methods use a pre-specified disturbance scenario to distribute the load increases for stressing the power system, i.e., the extra reactive power demands are added to each participating bus according to a given distribution. Different disturbance modes will stress the power system towards different critical points, and the conventional methods therefore cannot provide a well-defined voltage stability index.

Consider an N-Bus Power System with Bus-1 as the swing bus. By applying the de-coupling method, the active and reactive power flow equations, around an initial operating point, can be expressed by:

$$P_{Gi} = P_{Li} + \sum_{j=1}^{N} u_i u_j Y_{ij} \cos(\delta_i - \delta_j - \phi_{ij}) \quad i = 2, 3, \ldots, N \tag{1a}$$

$$Q_{Gi} = Q_{Li} + \sum_{j=1}^{N} u_i u_j Y_{ij} \sin(\delta_i - \delta_j - \phi_{ij}) \quad i = 2, 3, \ldots, N \tag{1b}$$

where u_i/δ_i is the ith node complex voltage, Y_{ij}/ϕ_{ij} is the (i, j)th entry of the power system admittance matrix, P_{Gi} and P_{Li} and Q_{Gi} and Q_{Li} respectively denote the active and reactive power generations and load demands at the ith node.

Suppose that a certain amount of extra reactive power loads $\sum_i \Delta Q_{Li}$ is imposed to a given area of the power system, with ΔQ_{Li} as the increment at Bus-i. Each individual ΔQ_{Li} can be related to the total increment via a participating factor: $\Gamma = [\gamma_1, \gamma_2, \ldots, \gamma_N]$ ($\sum_i \gamma_i = 1$). Thus while $\Delta Q_{Li} = \gamma_i Q_M$ is added to a certain bus-bar, the total load increment is calculated by $\sum_i \gamma_i Q_M = Q_M \sum_i \gamma_i = Q_M$, where Q_M is the parameter to be maximized in searching for the reactive power margin. Similarly, an SVC placement can be represented by a vector $\Xi = [\xi_1, \xi_2, \ldots, \xi_N]$ ($\sum_i \xi_i = 1$), where $\sum_i Q_{Si} = \sum_i \xi_i Q_{SVC} = Q_{SVC}$ with the Q_{Si} as the SVC allocation at Bus-i and the Q_{SVC} as the overall SVC capacity.

Using the participating factors, the reactive power margin of a power system can be easily assessed in terms of system VAR reservation under the given disturbance scenario and SVC placement, which can be evaluated through solving the following optimization problem:

$$\text{To maximize} \quad Q_M \tag{2}$$

$$\text{Subject to} \quad -P_{Gi} + P_{Li} + \Delta P_{Li} + \sum_{j=1}^{N} v_i v_j Y_{ij} \cos(\delta_i - \delta_j - \phi_{ij}) = 0 \tag{3}$$

$$-Q_{Gi} - Q_{Si} + Q_{Li} + \gamma_i Q_M + \sum_{j=1}^{N} u_i u_j Y_{ij} \sin(\delta_i - \delta_j - \phi_{ij}) = 0 \tag{4}$$

$$Q_{Gi}^{\min} \le Q_{Gi} \le Q_{Gi}^{\max} \tag{5}$$

$$0 \le Q_{Si} \le \xi_i Q_{SVC} \tag{6}$$

$$u_i^{\min} \le u_i \le u_i^{\max} \tag{7}$$

$$a_i^{\min} \le a_i \le a_i^{\max} \tag{8}$$

where the active and reactive power equation constraints are referred to Bus-2 to Bus-N ($i = 2, 3, \ldots, N$, except for the swing bus), a_i is the tap position of a load tap-changing (LTC) transformer. Since it is inappropriate to assume a constant voltage or a constant VAR support for each of the generator (condenser) and SVC nodes, say the ith bus, both u_i and Q_{Gi} (or Q_{Si}) are not specified. In the optimization, constraints to these three variables in addition to the tap positions (a_i) are represented by the two-side inequalities (5)–(8). The unknowns of the optimization are the node voltages $\{u_i/\delta_i\}$, the VAR generations $\{Q_{Gi}\}$ and $\{Q_{Si}\}$, the tap positions $\{a_i\}$, and the parameter Q_M, the critical VAR increase. As shown in (6), the allocated SVC support $\xi_i Q_{SVC}$ at each selected bus may not be fully engaged due to the voltage constraint.

It is known that voltage stability is closely related to the viability of a power system in reactive power support whereas the angle stability as well as the angle delta is mainly affected by the active power generation and transmission. During stressing the power system for voltage stability analysis and the pertinent SVC placement, consequently, the active power load at each bus-bar is assumed unchanged ($\Delta P_{Li} = 0$) in one of the case studies presented in the paper. For a more accurate estimation of the voltage stability margin, however, the paper also takes into account the increase of active power demands in the loadablity analysis, with each ΔP_{Li} being calculated in accordance with the reactive power load increment and the power factor:

$$\Delta P_{Li} = pf_i * \lambda_i Q_M \Big/ \sqrt{1 - pf_i^2} \tag{9}$$

where pf_i is the power factor obtained from the original power demands at each node.

Obviously, the worst-case VAR margin corresponds to the smallest VAR demand required to drive the power system into voltage instability. Such a margin is uniquely associated with the most critical point of voltage stability [6]. By performing a systematic search, the worst-case VAR margin of the power system can be obtained by:

To minimize Q_M through searching for the worst participating factors set Γ (10)

Subject to Q_M is the solution of (2)–(8) (11)

$$\gamma^{\min} \le \gamma_i \le \gamma^{\max} \tag{12}$$

$$\sum_i \gamma_i = 1 \tag{13}$$

To ensure feasibility, γ_i, i.e., each entry of the participating factor set, is limited by its upper and lower bounds. Once the worst-case VAR margin Q_M^* is solved, the accompanied participating factor set Γ^* indicates the most severe disturbance scenario during which the weakest bus-bars will be imposed the largest portion of the load increment. Consequently, the bus-bar corresponding to the largest worst-case participating factor should be chosen as the weakest bus-bar. Other smaller participating factors also contain useful information for demonstrating the relative strengths of bus-bars against the worst-case VAR disturbance.

3. SVC placement

SVCs are usually installed in heavily loaded areas to alleviate stressed power systems. On such a basis, the SVC planning can be modeled by a problem of assigning the appropriate capacity to the selected bus-bars of a power system so as to reinforce the system under the most critical operation conditions. However, the worst-case disturbance scenario denoted by Γ^*, in general, will be different under different SVC placements. As a result, the proposed optimal SVC placement can only be obtained through solving a three-level optimization problem:

(i) Maximizing Q_M for a given SVC placement (determined by the Ξ) and a disturbance scenario (determined by the Γ) to evaluate the VAR margin.
(ii) Searching for the participating factor set Γ^* leading to the minimum (worst-case) VAR margin under a certain SVC compensation Ξ.
(iii) Seeking the optimal SVC placement Ξ^* that maximizes the worst-case VAR margin.

The SVC planning, due to the three-level optimization, will be extremely difficult, if not impossible, to solve. For a practical SVC planning, the optimization problem should be significantly simplified. It appears that the Γ^* can be estimated from Γ_0^* (the normalized critical participating factor before installing the SVC), the overall SVC capacity Q_{SVC} and the candidate SVC placement Ξ:

$$\Gamma^* \approx \left(\Gamma_0^* - \frac{Q_{SVC}}{Q_{SVC} + Q_G}\Xi\right) \tag{14}$$

where Q_G is the total maximum reactive power support before the SVC installation. The estimated critical disturbance scenario is further processed by a repairing program to make it conform to the constraints as given in (12) and (13). Eq. (14) shows that the estimated most critical participation factor set, while based on the Γ_0^*, is affected by the SVC compensation at each bus-bar. The SVC compensation will decrease the corresponding participating factor since the strength of the node has been increased. The influence of the SVC placement is proportional to the overall compensation capacity compared with the total VAR reserve.

By taking the approximation made in (14), the three-level optimization can be simplified into 2-level optimization problem. The original worst participating factor set and the VAR reserve, i.e., the Γ_0^* and Q_{M0}^* can be first evaluated before installing SVC by solving (10)–(13) with $Q_{SVC} = 0$ in (2)–(8). Then, in the first sub-problem, the worst-case VAR margin is calculated by solving (2)–(8) with the estimated Γ^*. In the main sub-problem, the optimal SVC planning is sought to maximize the worst-case VAR margin and the other sub-objectives summarized below.

The effectiveness of each proposed SVC placement, for voltage stability reinforcement, should be assessed by its performance in

(i) increasing the worst-case power system reactive margin,
(ii) reducing the total real power losses,
(iii) preventing low voltage profiles,
(iv) minimizing the cost of the SVC devices, and
(v) maximizing the $N-1$ voltage stability under a normal disturbance scenario.

Thus, upon obtaining the reactive margin and the corresponding critical point, i.e., the solution of (2)–(8), two of the other sub-objective functions can be evaluated accordingly. The total real power loss denoted by P_{Loss} is calculated by:

$$P_{Loss} = \sum_{i,j=1,2,l...,N} [u_i^2 + u_j^2 - 2u_iu_j\cos(\delta_i - \delta_j)]Y_{ij}\cos\phi_{ij} \tag{15}$$

The P_{Loss} provides a measure to the real power loss when the power system being heavily loaded towards the critical point.

In maximizing the reactive margin, the minimum voltage magnitudes of all buses have been ensured by introducing constraints in the optimization (7). Furthermore, the average voltage is taken as one of the criteria in assessing the performance of the SVC reinforcement:

$$U_{Ave} = \underset{i\in S_u}{average}\{u_i\} \tag{16}$$

where S_U is the set of participating bus-bars. Without this criterion, the evaluated critical point and the VAR margin may give misleading result as mentioned earlier. The P_{Loss} and U_{Ave} in (15) and (16) are calculated with the data $\{u_i, \delta_i, a_i\}$ of the power system at the critical point. The optimal SVC placement should minimize P_{Loss} and, at the same time, maximize U_{Ave}.

The cost of SVC compensation can be estimated by the capacity and location of each selected SVC node. In this paper, the SVC scheme cost E_{Cost} is determined by the number of SVC nodes only. For a total compensation capacity, in general, the more the number of the SVC nodes, the higher the SVC system will cost.

For each candidate SVC placement, the $N-1$ reactive power margin will be calculated by assuming a typical disturbance scenario related to the original distribution of reactive power demands. A search program may be performed to find the most critical line to trip off.

To obtain a single objective function, the multi-objective optimization addressed above can be transformed to an optimization problem with a single objective function by virtue of assigning each sub-objective function with a fuzzy goal. The fuzzy goals are quantified by selected membership functions and reference membership values. For the sub-objective functions to be maximized or minimized, the membership functions shown in Fig. 1 are introduced, where $U(f_i)$, $i = 1$–4 is the membership values of Q_M, P_{Loss}, U_{Ave}, or E_{Cost} with f_i^0 and f_i^1 respectively as the unacceptable- and desirable-level. To achieve an overall optimal SVC compensation with respect to all the four sub-objectives, therefore, the SVC placement is transformed into a fuzzy decision problem described by the following optimization model:

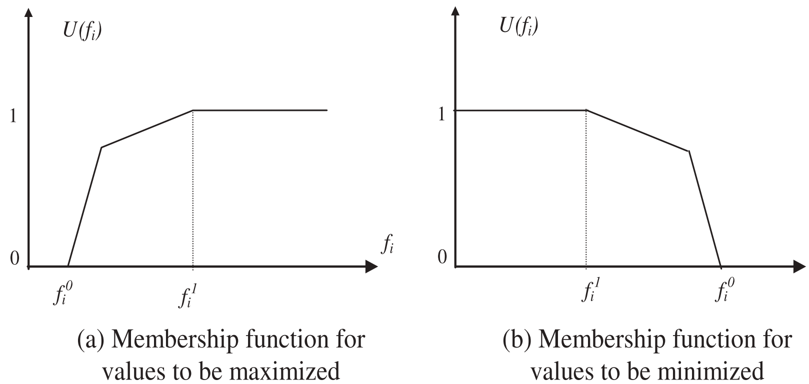

Fig. 1. Fuzzy performance index: f_i represents Q_M, P_{Loss}, V_{Ave}, or E_{Cost}; f_i^0 is an unacceptable level, f_i^1 is a desirable level.

To maximize $F = \min_{i=1,2,3,4}\{U(f_i)\}$ by searching for the

$$\text{optimal SVC placement } \Xi \tag{17}$$

Subject to

$$Q_M \text{ is the solution of (2)–(8) for estimated } \Gamma^* \tag{18}$$

$$\xi_i : \xi_{\min} : \Delta\xi : \xi_{\max}, \quad i = 2, 3, \ldots, N \tag{19}$$

$$\sum \xi_i = 1 \tag{20}$$

where $\xi_{\min}$ and $\xi_{\max}$ are the lower and upper bounds of the SVC capacity assigned for each single bus, and $\Delta\xi$ is the step size of the compensation adjustment. The decision variables of the optimization is the vector $\Xi = [\xi_1, \xi_2, \ldots, \xi_N]$. In the above optimization, all SVC nodes are treated as PV nodes.

Optimization (17)–(20) is to seek the optimal SVC placement in terms of reactive power margin, real power losses, average voltages and cost of the SVC scheme. The thereby obtained SVC placement is further checked against the $N-1$ stability criterion. With the candidate SVC reinforcement, the power system losing a linkage should possess a certain reactive power margin under a normal disturbance scenario. In the proposed SVC planning, the $N-1$ reactive power margin Q_{N-1} is evaluated by tripping a critical linkage and stressing the power system with the disturbance proportional to the original reactive power demands. In general, this $N-1$ reactive power margin is required to be larger than Q_M obtained in (17)–(20), so that the Q_M can provide a reliable estimation of voltage stability margin, under either the worst-case disturbance scenario or an incidence caused by tripping out of a critical linage. Fig. 2 outlines the whole course of the SVC planning.

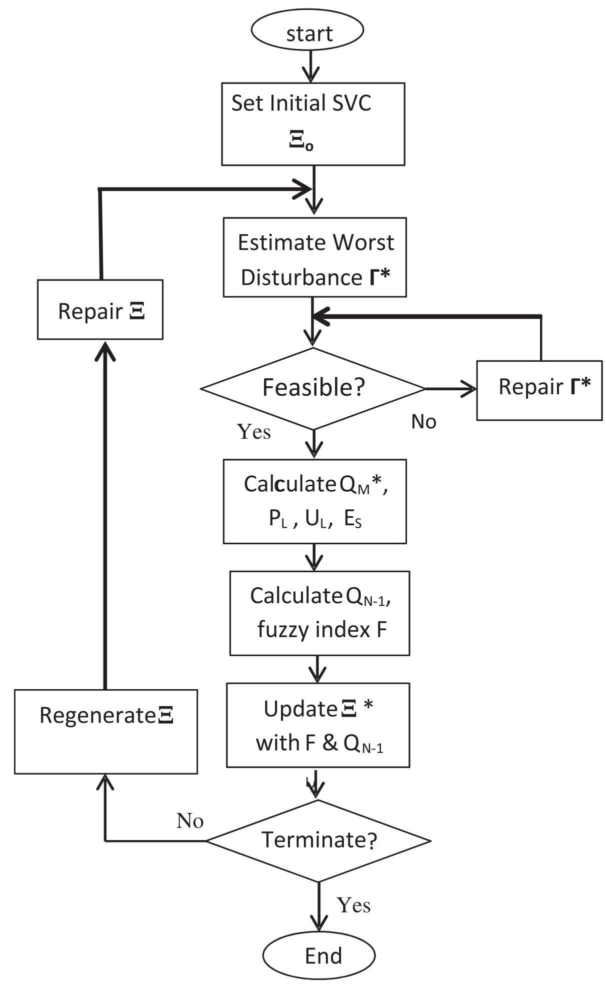

Fig. 2. Optimal SVC planning scheme.

4. Optimization techniques

In light of the discussion in the preceding section, the challenge of SVC planning lies in the evaluation of the reactive margin whereas all the other objectives can be obtained accordingly.

4.1. Lagrange multiplier method

The optimization scheme adopts Lagrange multiplier method for the computation of the VAR margin. For each ith node the unknowns of the optimization are: the node voltage u_i/δ_i (u_i and δ_i), the reactive generation Q_{Gi} and Q_{Si}, and the tap position a_i, in conjunction with the reactive power margin Q_M over the concerned region. The algorithm removes each of the two-side constraints by introducing the multiplier. Expressing the vector of the variables to be solved as $X = [U^T, \Delta^T, Q_G^T, Q_S^T, a^T, Q_M]^T$, the equality constraints of (3) and (4) as $E_i = 0$ ($i = 1, 2, 3, \ldots, 2N-2$) and the two-side inequality constraints as $\alpha_j \leqslant G_j \leqslant \beta_j$ ($j = 1, 2, \ldots, N_{IE}$, with N_{IE} as the number of inequality constraints), the augmented Lagrange is obtained by converting all the inequality constraints into the equality ones. The modified optimization problem can then be solved as a sequence of unconstrained problems [17].

4.2. Messy genetic algorithm for SVC planning

Obviously, normal optimization techniques are insufficient in searching for the optimal SVC placement described by (17)–(20). A GA based method is adopted for the optimization. During the GA search, each candidate solution denoted by Ξ is encoded with a binary string termed a chromosome [18]. Since the number of bus-bars selected for the SVC installation is not fixed, the optimization uses a messy genetic algorithm [19], while a normal GA method is used for the worst-case reactive power margin problem (10)–(13).

A particular scheme is proposed for the messy encoding, where the chromosome length is variable and each gene is represented by a pair of numbers, i.e., the location of a SVC node and the corresponding allocation of the SVC capacity. With this encoding method, genes can be arranged in any order. A set of candidates at a given searching stage (generation) forms the population. With a randomly selected initial population conforming to the constraints (19) and (20), the GA carries out the optimization process. In the messy GA method, a single point crossover operation adopted. Whilst the crossover point can be arbitrarily chosen from the first chromosome, the point at the second chromosome is determined at the corresponding position but in an arbitrary gene, as illustrated in Fig. 3. A uniform mutation operation is used as done by many normal GA methods.

Because the chromosome for each SVC bus is randomly distributed, the messy GA will not introduce any bias to any particular bus-bars. Apart from this, the messy GA method can effectively avoid pre-mature termination. In the developed genetic algorithm, the size of the population is set 50 for searching the worst-case disturbance and 40 for the optimal SVC placement, the crossover rate is 0.6, and the mutation rate is 0.01. In addition, the tournament selection is used in the reproduction and the tournament size is 2. In the GA search, the best candidate (the SVC placement having highest fuzzy index and meeting the $N-1$ criterion) is always recorded but not included in the next generation at early stage to further prevent from the pre-mature termination.

Due to the adoption of a variable length, the messy GA approach may suffer under- or over-specified string problems. In the SVC placement, the messy GA may cause the total SVC installation less than the total given capacity (under specification), or a single node is allocated with a different SVC capacity (over specification). In the proposed SVC planning, the ambiguity in the latter is solved on the basis of a first-come, first-served rule while the SVC shortage in the former is solved by randomly allocating the absent SVC capacity to the un-selected bus-bars. In addition, a repairing algorithm is applied in case any resulted offspring in a new generation violates the constraints imposed on the SVC placement.

5. Simulation and discussions

As shown in Fig. 4, the IEEE 30-Bus System is used in the case study [20]. In this paper, the participating nodes include all the load buses. Assuming that the total capacity of the SVCs to be installed is 1.0 p.u., the compensation assigned at each selected node is within the limits of 0.1 p.u. (ξ_{min} = 1/10) and 1.0 p.u. (ξ_{max} = 1), and in a multiple of 0.1 p.u. ($\Delta\xi$ = 1/10).

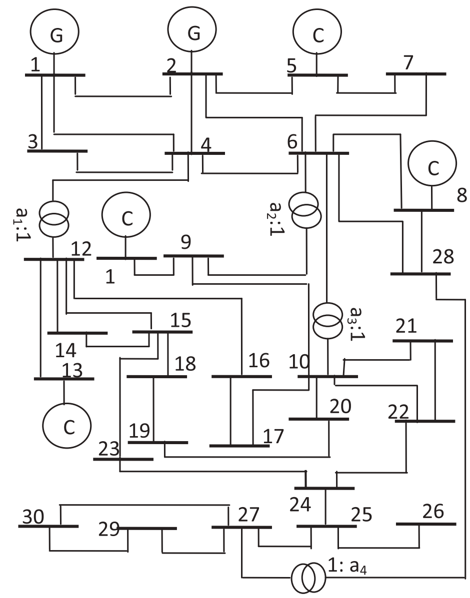

Fig. 4. Study power system (IEEE 30-Bus System).

5.1. Original worst-case VAR margin

Using the method described in Section 2, the worst-case VAR margin and the corresponding participating factor set are evaluated. As shown in Table 1, the $Q_M^* = 0.1494$ and each entry of Γ_0^* is given in the right most column. Since $\gamma_{26} = \gamma_{29} = \gamma_{30} = 1$ is the largest participating factor, Bus-26, 29 and 30 are identified as the weakest bus-bars (Bus-30 can be regarded as the weakest since the voltage is the lowest). The other weak bus-bars include Bus-16 and Bus-23. The worst-case VAR margin and the accompanied participating factors can be used to find the bus-bar most vulnerable to voltage collapse. Fig. 5 shows the GA search for the most critical disturbance scenario. In general, the optimization converged in less than 80 generations.

The above case study assumes that the active power demand at each node keeps unchanged based on the consideration that the voltage stability is mainly affected by the reactive power load and support. It is nonetheless necessary to study the influence of extra active power demands to the reactive power margin and the worst-case disturbance scenario. By employing (9), the corresponding incremental active power load is imposed at each node and the same search is carried out to estimate the reactive power margin and the participating factors. The results are given in Table 2. It can be seen that the reactive margin is much smaller now while the worst-case disturbance scenario (the participating

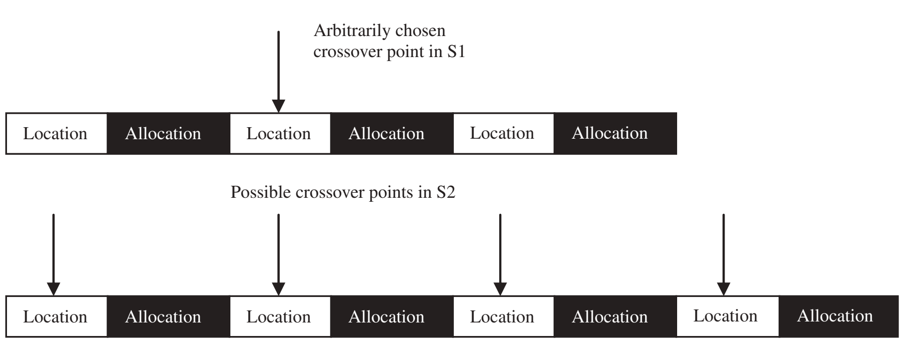

Fig. 3. Crossover operation of the messy GA.

Table 1
Worst-case VAR margin of the IEEE 30-Bus System ($\Delta P_L = 0$).

Node	Q_{Gi} (p.u.)	u_i (p.u.)	δ_i (°)	a_i (100%)	γ_i
1	–	1.0600	0	–	–
2	0.5000	1.0298	−0.0930	–	−0.2000
3	–	1.0020	−0.1329	–	0.1041
4	–	0.9904	−0.1645	0.9236	−0.2000
5	0.4000	0.9903	−0.2540	–	−0.2000
6	–	0.9793	−0.1946	0.8500 0.8855	0
7	–	0.9763	−0.2289	–	−0.2000
8	0.4000	0.9768	−0.2078	–	−0.2000
9	–	1.1066	−0.2471	–	0
10	–	1.1093	−0.2736	–	−0.2000
11	0.2400	1.1500	−0.2471	–	0
12	–	1.1208	−0.2602	–	−0.2000
13	0.2400	1.1500	−0.2602	–	0
14	–	1.1092	−0.2767	–	−0.2000
15	–	1.1005	−0.2763	–	−0.2000
16	–	1.1022	−0.2678	–	0.4677
17	–	1.1040	−0.2755	–	−0.2000
18	–	1.1007	−0.2897	–	−0.2000
19	–	1.1002	−0.2931	–	−0.2000
20	–	1.1032	−0.2897	–	−0.2000
21	–	1.0927	−0.2806	–	−0.2000
22	–	1.0910	−0.2801	–	0
23	–	1.0702	−0.2772	–	0.4282
24	–	1.0538	−0.2803	–	−0.2000
25	–	0.9793	−0.2575	–	0
26	–	0.8956	−0.2226	–	1.0000
27	–	0.9775	−0.2555	–	0
28	–	0.9562	−0.1993	0.8500	0
29	–	0.8740	−0.2374	–	1.0000
30	–	0.8500	−0.2512	–	1.0000
Q_M^* (p.u.)				0.1494	
P_{Loss}^* (p.u.)				0.0730	
U_{Ave}^* (p.u.)				1.0394	

Table 2
Worst-case VAR margin of the IEEE 30-Bus System ($\Delta P_L \propto pf$).

Node	Q_{Gi} (p.u.)	u_i (p.u.)	δ_i (°)	a_i (100%)	γ_i
1	–	1.0600	0	–	–
2	0.5000	1.0185	−0.1063	–	−0.2000
3	–	0.9910	−0.1539	–	−0.2000
4	–	0.9763	−0.1915	0.9074	0.2627
5	0.4000	0.9654	−0.2911	–	0.4836
6	–	0.9631	−0.2299	0.8500 0.8791	0
7	–	0.9557	−0.2640	–	−0.2000
8	0.4000	0.9598	−0.2459	–	−0.2000
9	–	1.1066	−0.2790	–	0
10	–	1.1086	−0.3039	–	−0.2000
11	0.2400	1.1500	−0.2790	–	0
12	–	1.1208	−0.2829	–	−0.2000
13	0.2400	1.1500	−0.2829	–	0
14	–	1.1103	−0.2950	–	−0.2000
15	–	1.1015	−0.3002	–	−0.2000
16	–	1.1102	−0.2943	–	−0.2000
17	–	1.1053	−0.3038	–	−0.2000
18	–	1.0992	−0.3058	–	−0.2000
19	–	1.0978	−0.3091	–	−0.2000
20	–	1.1008	−0.3076	–	−0.2000
21	–	1.0932	−0.3151	–	−0.2000
22	–	1.0922	−0.3165	–	0
23	–	1.0776	−0.3214	–	0.2537
24	–	1.0602	−0.3411	–	−0.2000
25	–	1.0005	−0.3957	–	0
26	–	0.9446	−0.4191	–	1.0000
27	–	0.9936	−0.4185	–	0
28	–	0.9386	−0.2519	0.8500	0
29	–	0.8895	−0.5204	–	1.0000
30	–	0.8500	−0.5803	–	1.0000
Q_M^* (p.u.)				0.0455	
P_{Loss}^* (p.u.)				0.0776	
U_{Ave}^* (p.u.)				1.0390	

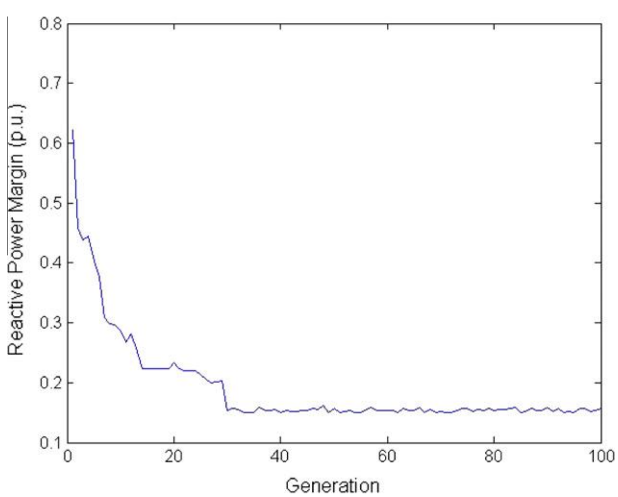

Fig. 5. GA search for the worst-case disturbance scenario.

factor) is very similar to that obtained without introducing the incremental active power loads.

It should be pointed out that the case study with extra active power loads is based on the assumption that Bus-1 (the swing bus) can pick up the entire extra active power load imposed on the node. Under the identified critical disturbance, however, the active power injection at Bus-1 exceeds 2.6 p.u. (260 MW) given by the specification of the study system. By introducing this constraint in the optimization (2)–(8), the reactive power margin will be a negative value, i.e., the system would be unable to maintain even the original loading level should the load demands obey the identified worst-case distribution.

5.2. Optimal SVC scheme

The most critical participating factors obtained in the two case studies are very similar, verifying that the reactive power margin and the voltage stability are not much influenced by the active power demands. Thus, based on the Γ_0^* obtained in the first case study, the proposed messy GA based algorithm is applied to evaluate the optimal SVC placement such that the fuzzy satisfying index is maximized. With the Γ_0^*, the worst case disturbance is estimated for each SVC candidate and the corresponding reactive margin and the other sub-objectives are calculated. The simulation results are shown in Table 3. Under the optimal SVC placement, Bus-26, Bus-29 and Bus-30 are selected as the SVC sites with the capacity assignment respectively as 0.3 p.u., 0.3 p.u. and 0.4 p.u. Under the SVC reinforcement, the performance of the power system has been significantly improved from $Q_M^* = 0.1494$ p.u., $P_{Loss}^* = 0.0776$ p.u., and $U_{Ave}^* = 1.0390$ p.u., to $Q_M^* = 0.5686$ p.u., $P_{Loss}^* = 0.08312$ p.u., and $U_{Ave}^* = 1.0486$ p.u. The right-most column lists the estimated participating factors corresponding to the most critical disturbance scenario.

It is observed that the three weakest bus-bars are selected as the SVC nodes. Furthermore, the line loss is slightly higher than the original value and the improvement of the reactive margin is much lower compared with the capacity of the installed SVCs. While the first observation seems to match what has been expected, it is not always the case since the strength of each node can be quite different before and after the SVC placement. The

Table 3
Reactive margin, power losses, load voltages under optimal SVC reinforcement.

Node	Q_{Gi} (p.u.)	u_i (p.u.)	δ_i (°)	a_i (100%)	γ_i[b]
2	0.5000	1.0357	−0.1710	–	−0.1829
3	–	1.0158	−0.1806	–	0.1212
4	–	1.0108	−0.2241	0.9733	−0.1829
5	0.4000	1.0155	−0.3243	–	−0.1829
6	–	1.0027	−0.2598	0.8500 0.9304	0
7	–	1.0042	−0.2969	–	−0.1829
8	0.4000	1.0022	−0.2730	–	−0.1829
9	–	1.1066	−0.3148	–	0
10	–	1.1253	−0.3414	–	−0.1829
11	0.2400	1.1500	−0.3148	–	0
12	–	1.1208	−0.3236	–	−0.1829
13	0.2400	1.1500	−0.3236	–	0
14	–	1.1221	−0.3462	–	−0.1829
15	–	1.1102	−0.3434	–	−0.1829
16	–	1.0891	−0.3268	–	0.4848
17	–	1.1151	−0.3412	–	−0.1829
18	–	1.1329	−0.3651	–	−0.1829
19	–	1.1374	−0.3698	–	−0.1829
20	–	1.1384	−0.3654	–	−0.1829
21	–	1.1100	−0.3493	–	−0.1829
22	–	1.1071	−0.3485	–	0
23	–	1.0577	−0.3343	–	0.4454
24	–	1.0606	−0.3459	–	−0.1829
25	–	0.9694	−0.3179	–	0
26	0.3000[a]	0.8500	−0.2600	–	0.9092
27	–	0.9770	−0.3202	–	0
28	–	0.9766	−0.2635	0.8500	0
29	0.3000[a]	0.8596	−0.2944	–	0.9092
30	0.4000[a]	0.8580	−0.3211	–	0.8732
Q^*_M (p.u.)				0.5686	
P^*_{Loss} (p.u.)				0.0831	
U^*_{Ave} (p.u.)				1.0486	
Q^*_{N-1} (p.u.)[c]				1.3182	

[a] Q_{Si}.
[b] Estimated worst-case disturbance scenario.
[c] $N-1$ reactive power margin.

higher real power loss is due to the much higher loading level at the critical point after the SVC reinforcement. The last observation can be explained by the characteristics of the worst-case disturbance scenario. In addition, the SVC placement is a multi-objective optimization and is assessed by the fuzzy performance index and the $N-1$ security criterion, instead of a single sub-objective.

The convergence performance of the main sub-problem is illustrated in Fig. 6, where each point of the curve represents the fuzzy performance index value.

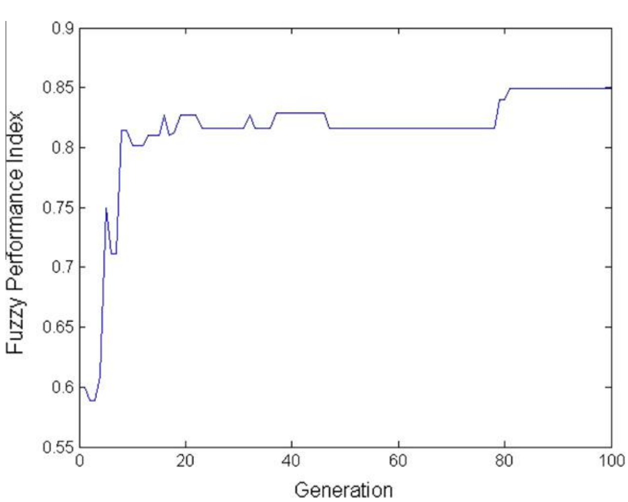

Fig. 6. GA convergence plot for optimal SVC placement.

5.3. $N-1$ reactive power margin

For $N-1$ stability analysis, one critical linkage between Bus-1 and Bus-2 was selected in the case study. It is assumed that one of the two feeders between the two generation nodes is tripped out. Before the SVC installation, the original system had an $N-1$ reactive power margin of 0.7309 p.u. under a normal disturbance (extra loads proportional to the original power demands). With the SVC reinforcement, the $N-1$ reactive power margin has been increased to 1.3182 p.u. that is much higher than the worst-case reactive power margin (0.5686 p.u.). In the GA searching for the optimal SVC placement, the best candidate at each generation is checked again the $N-1$ security criterion and only those that satisfy the requirements $Q_{N-1} > Q_M$ and $Q_{N-1} > Q_{SVC}$ will be kept.

The selection of the linkage to trip off in evaluating the $N-1$ reactive power margin is based on the consideration to the influence of the linkage to the entire power system. In fact, the most critical linkage in terms of reactive power margin can be easily identified by repeatedly solving the optimization (2)–(8) under the given normal disturbance and with one of the candidate linkages being tripped off each time.

6. Conclusions

The paper investigates the loadability of power systems. With or without active power load increment in stressing the study system, a voltage stability assessment defined by the worst-case reactive power margin is performed. Based on this assessment, an optimization scheme using the messy GA and the Lagrange multiplier techniques have been developed for SVC planning. The scheme optimizes the performance of an SVC scheme with respect to the five identified sub-objectives. The fuzzy satisfying method provides a good tradeoff for planners' requirements related to voltage stability enhancement. While focusing upon system performance under the most critical conditions and the $N-1$ security margin, the optimization takes into account the reactive limits of generators, allowable voltage working ranges, lower and upper transformer tap limits, the influence of the active power loads, the feasibility of disturbance scenario, and other system constraints and nonlinear effects. As a result, the proposed optimization scheme provides a more accurate and reliable guidance in SVC planning. By estimating the most critical disturbance scenario with the original operation conditions and each candidate SVC placement, the complex SVC planning has been greatly simplified.

References

[1] Prada RB, Souza LJ, Sousa LAP. The need for a new constraint on voltage/reactive power studies to ensure proper voltage control. Int J Electr Power Energy Syst 2002;24(7):535–40.
[2] Thukaram D, Parthasarathy K, Khincha HP, Narendranath Udupa, Bansilal A. Voltage stability improvement: case studies of Indian power networks. Electr Power Syst Res 1998;44(1):35–44.
[3] Taylor CW. Recording and analyzing the July 2 cascading outage [Western USA power system]. IEEE Comput Appl Power 1997;10(1):26–30.
[4] Lee BH, Lee KY. A study on voltage collapse mechanism in electric power system. IEEE Trans Power Syst 1991;6(3):966–74.
[5] Sauer PW, Lesientre BC, Pai MA. Maximum loadability and voltage stability in power system. Int J Electr Power Energy Syst 1993;15(3):145–54.
[6] Lõf P-A, Andersson G, Hill DJ. Voltage stability indexes for stressed power system. IEEE Trans Power Syst 1993;8(1):326–34.
[7] Chang CS, Huang JS. Worst-case identification of reactive power margin and local weakness of power systems. Electr Power Syst Res 1998;44(2):77–83.
[8] Parker CJ, Morrison IF, Sutanto D. Application of an optimization method for determine the reactive margin from voltage collapse in reactive power planning. In: 1995 IEEE/PES summer meeting, 586-8 PWRS, Portland (OR); July 23–27, 1995.
[9] Cutsem TV. A method to compute reactive power margins with respect to voltage collapse. IEEE Trans Power Syst 1991;6(1):145–53.

[10] Huang JS, Negnevitsky M. Optimal SVC placement for voltage stability reinforcement of power systems under critical operation conditions. Int J Power Energy Syst 2011;31(3).

[11] El-Araby El-said El-sayed, Yorino Naoto, Sasaki Hiroshi. A two level hybrid GA/SLP for FACTS allocation problem considering voltage security. Int J Electr Power Energy Syst 2003;25(4):327–35.

[12] Wang Y, Chen H, Zhou R. A nonlinear controller design for SVC to improve power system voltage stability. Int J Electr Power Energy Syst 2000;22(7):463–70.

[13] Johansson Stefan G, Daalder Jaap E, Popović Dragana, Hill David J. Avoiding voltage collapse by fast active power rescheduling. Int J Electr Power Energy Syst 1997;19(8):501–9.

[14] Jwo WS, Liu CW, Liu CC, Hsiao YT. Hybrid expert system and simulated annealing approach to optimal reactive planning. IEE Proc Gener Trans Distrib 1995;142(4):381–5.

[15] Hsiao YT, Chiang HD, Liu CC, Chen YL. A computer package for optimal multi-objective VAR planning in large scale power systems. IEEE Trans Power Syst 1994;9(2):668–76.

[16] Mansour Y, Xu W, AlVARado F, Rinzin C. SVC placement using critical modes of voltage stability. In: IEEE PICA conference, Scottsdale (AZ, USA); May 4–7, 1993. p 131–7.

[17] Bertsekas DP. Constrained optimization and Lagrange multiplier methods. Academic Press; 1982.

[18] Michalewicz Z. Genetic algorithms + data structures = evolution programs. Springer-Verlag; 1994.

[19] Jain LC. Evolutionary computation. CRC Press; 2000.

[20] http://www.ee.washington.edu/research/pstca/pf30/pg_tca30bus.htm.